

Investigation of the nanodomain structure formation by piezoelectric force microscopy and Raman confocal microscopy in LiNbO₃ and LiTaO₃ crystals

V. Ya. Shur, P. S. Zelenovskiy, M. S. Nebogatikov, D. O. Alikin, M. F. Sarmanova et al.

Citation: *J. Appl. Phys.* **110**, 052013 (2011); doi: 10.1063/1.3623778

View online: <http://dx.doi.org/10.1063/1.3623778>

View Table of Contents: <http://jap.aip.org/resource/1/JAPIAU/v110/i5>

Published by the [American Institute of Physics](#).

Related Articles

Enhanced piezoelectric properties of (Na_{0.5+y+z}K_{0.5-y})(Nb_{1-x}Tax)O₃ ceramics
Appl. Phys. Lett. **101**, 012902 (2012)

Multiferroic response of nanocrystalline lithium niobate
J. Appl. Phys. **111**, 07D907 (2012)

Non-radiative complete surface acoustic wave bandgap for finite-depth holey phononic crystal in lithium niobate
Appl. Phys. Lett. **100**, 061912 (2012)

Investigation of dielectric and electrical properties of Mn doped sodium potassium niobate ceramic system using impedance spectroscopy
J. Appl. Phys. **110**, 104102 (2011)

Determination of depolarization temperature of (Bi_{1/2}Na_{1/2})TiO₃-based lead-free piezoceramics
J. Appl. Phys. **110**, 094108 (2011)

Additional information on *J. Appl. Phys.*

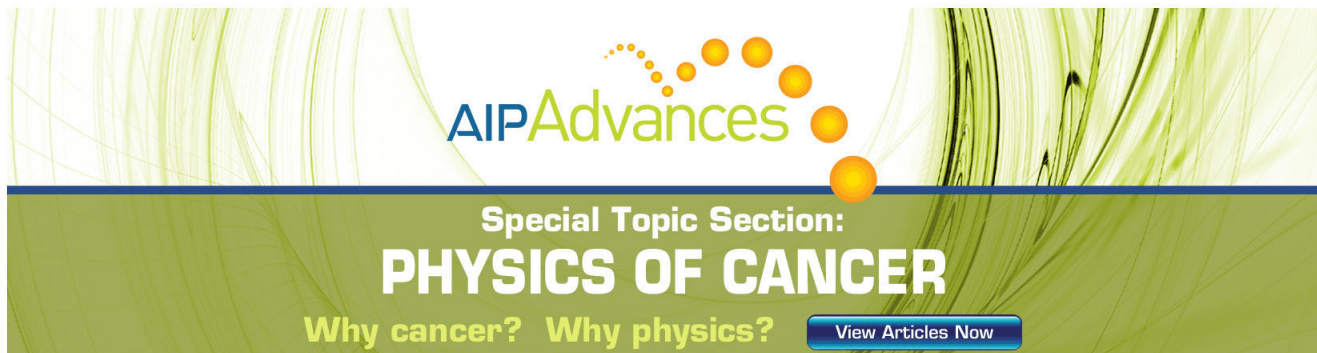
Journal Homepage: <http://jap.aip.org/>

Journal Information: http://jap.aip.org/about/about_the_journal

Top downloads: http://jap.aip.org/features/most_downloaded

Information for Authors: <http://jap.aip.org/authors>

ADVERTISEMENT



AIP Advances

Special Topic Section:
PHYSICS OF CANCER

Why cancer? Why physics? [View Articles Now](#)

Investigation of the nanodomain structure formation by piezoelectric force microscopy and Raman confocal microscopy in LiNbO₃ and LiTaO₃ crystals

V. Ya. Shur,^{a)} P. S. Zelenovskiy, M. S. Nebogatikov, D. O. Alikin, M. F. Sarmanova, A. V. Ilevlev, E. A. Mingaliev, and D. K. Kuznetsov
Ferroelectric Laboratory, Institute of Physics and Applied Mathematics, Ural State University, 620083 Ekaterinburg, Russia

(Received 14 February 2011; accepted 23 May 2011; published online 2 September 2011)

Piezoelectric force microscopy (PFM) and Raman confocal microscopy have been used for studying the nanodomain structures in congruent LiNbO₃ and LiTaO₃ crystals. The high-resolution nanodomain images at the surface were observed via PFM. Raman confocal microscopy has been used for the visualization of the nanodomain structures in the bulk via layer-by-layer scanning at various depths. It has been shown experimentally that the nanodomain images obtained at different depths correspond to domain images at the polar surface obtained at different moments: the deeper the nanodomain, the earlier the moment. Such a correlation was applied for the reconstruction of the evolution of the domain structures with charged domain walls. The studied domain structures were obtained in highly non-equilibrium switching conditions realized in LiNbO₃ and LiTaO₃ via pulse laser irradiation and the electric field poling of LiNbO₃, with the surface layer modified by ion implantation. The revealed main stages of the domain structure evolution allow the authors to demonstrate that all geometrically different nanodomain structures observed in LiNbO₃ and LiTaO₃ appeared as a result of discrete switching. © 2011 American Institute of Physics. [doi:10.1063/1.3623778]

I. INTRODUCTION

The study of the nanodomain structures in lithium niobate [LiNbO₃ (LN)] and lithium tantalate [LiTaO₃ (LT)] with high spatial resolution is stimulated by the recent development of nanodomain engineering.^{1,2} The main target of nanodomain engineering is the manufacturing of stable tailored periodical or quasi-regular ferroelectric domain structures in order to improve the characteristics important for application.^{1,2} LN and LT are the most popular materials for nanodomain engineering. Periodically poled LN crystals (PPLN) are used for light frequency conversion based on a quasi-phase-matching effect.^{3–5} There are few experimental methods that allow one to study the domain structures in the bulk. Another important problem is the study of the domain forward growth, which is still the most mysterious stage of the domain evolution,^{6–9} because this stage is crucial for the creation of the precise periodic domain structures in LN and LT used for nonlinear optical devices.^{3–5}

The most popular method for domain study in LN and LT is based on selective chemical etching in hydrofluoric acid for domain revealing with subsequent visualization of the surface relief via optical, electronic, or scanning probe microscopy.¹⁰ But this is a partially destructive method, as it has been shown experimentally that the etching procedure leads to essential reconstruction of the domain structure.¹¹ The nanodomain structure is especially sensitive to this undesirable effect.

Piezoelectric force microscopy (PFM) allows one to study the nanodomain structures without preliminary etching with the best spatial resolution.^{12,13} Nevertheless, the method can be used for visualization of the domain structure, but at the crystal surface only.

The most popular nondestructive method for domain study is polarizing optical microscopy.¹⁴ In contrast to other methods, it allows one to observe the domains even in the bulk, but with comparatively low spatial resolution caused by the diffraction limit. Nevertheless, it is possible to visualize the long narrow domains with nanoscale widths.

It has been demonstrated recently that Raman confocal microscopy opens up new opportunities for the study of domain structure in LN crystals.^{15–17} This technique is based on the recording of the Raman spectra collected subsequently during scanning of the studied crystal. The change of the phonon modes in the vicinity of the domain walls in LN leads to local variation in the position and intensity of certain Raman lines.^{15–17} Similar effects were noted in LT.¹⁸ For visualization of the domain walls, the spatial dependence of the integrated intensity of the chosen Raman line obtained during two-dimensional (2D) scanning was converted into 2D digital arrays and represented in gray-scale or pseudo-color images.^{15–17} The proposed method is especially useful for the investigation of domain structures in the crystal bulk.¹⁷ Moreover, the spatial resolution of confocal microscopy is below the diffraction limit.

In the present work, we demonstrate the application of Raman confocal microscopy accompanied by PFM for studying the nanodomain kinetics through the visualization of various types of domain structures in the bulk of LN and LT crystals. PFM was used to obtain additional high resolution surface domain images.

II. EXPERIMENT

PFM measurements were realized by the Probe Nano Laboratory NTEGRA Aura (NT-MDT, Russia). Boron doped silicon cantilevers DCP11 (NT-MDT, Russia) with diamond-like conductive coated tips were used. The typical

^{a)}Author to whom correspondence should be addressed. Electronic mail: vladimir.shur@usu.ru.

value of the radius of the curvature of the tips was 70 nm as claimed by the manufacturer. The spring constant and the resonance frequency of the cantilevers used were about 7.5 N/m and 150 kHz, respectively. An ac modulation voltage $U_{mod}(t)$ (10 V, 12.3 kHz) was applied between the conductive tip and the bottom electrode in order to invoke the piezoelectric response of the surface. The signal from a scanning probe microscope (SPM) photodetector was analyzed using a lock-in amplifier SR-830 (Stanford Research Systems, USA). The spatial dependences of the piezoelectric response signal $Y_{PFM} = R \cdot \sin \theta$ obtained during 2D scanning, where R is an amplitude and θ is a phase of the response, were converted into 2D digital arrays and images.

We used a Probe NanoLaboratory NTEGRA Spectra (NT-MDT, Russia), which comprises a high resolution confocal scanning laser microscope, a Raman spectrometer, and a SPM. The Raman spectra were recorded in a $Z(x\bar{x})\bar{Z}$ configuration at room temperature within a 2D scanning with a step of 100 nm for obtaining the domain images at different depths in the bulk. The diode-pumped solid state laser (Cobolt AB, Sweden) with $\lambda = 473$ nm and a power of 50 mW was used as a pumping source. Laser focusing was performed with a $\times 100$ objective (NA = 0.95) mounted in the inverted microscope Olympus IX71. A diffraction grating of 1800 dash/mm with a spectral resolution of 1.2 cm^{-1} at $\lambda = 473$ nm was used for light decomposition. The estimated achieved spatial resolution was about 300 nm in the plane of the sample and about 500 nm in the vertical direction (depth).

It has been shown in LN that the integrated intensity of Raman lines around 580 and 870 cm^{-1} , corresponding to $E(\text{TO}_8)$ and $A_1(\text{LO}_4)$ phonon modes, respectively, change essentially in the vicinity of the domain walls: for $E(\text{TO}_8)$ it increases, and for $A_1(\text{LO}_4)$ it decreases.^{15,16} The measured changes of the integrated intensity allow us to visualize the domain structures by recording the Raman spectra in adjacent points during scanning over the sample. The spatial dependence of the integrated intensity of the chosen Raman line obtained during 2D scanning has been converted into 2D digital arrays and is represented in gray-scale or pseudocolor images. The approbation of the proposed technique was performed in PPLN.^{15–17}

In order to improve the image quality, we have applied a mathematical treatment of the Raman spectrum. The integrated intensity is sensitive to temporal and spatial variations of external conditions and the surface quality; we have shown that the parameter of “mass center frequency” $\omega_{MC} = \sum \omega_i I_i / \sum I_i$ calculated over the spectral range from 500 to 1000 cm^{-1} is less sensitive. This is the reason for using the spatial distribution of ω_{MC} for domain visualization in all presented images.

We have studied two types of nanodomain structures: (1) those produced by electric field poling in LN wafers with a Z^+ surface modified by the implantation of Ar ions, and (2) those formed in LN and LT as a result of pulsed irradiation by infrared (IR) laser.

The implantation of Ar ions in the Z^+ surface of 0.5-mm-thick Z-cut congruent lithium niobate (CLN) wafer (Crystal Tech., USA) was made in the Charged-particle Beams laboratory of the Institute of Electrophysics, UB RAS

(Ekaterinburg, Russia) with an energy of 40 keV and a total fluence of $9.4 \times 10^{16} \text{ cm}^{-2}$.

It has been shown that the polarization reversal in CLN with a modified surface layer leads to the self-organized formation of nanodomain patterns under the ineffective external screening of the depolarization field (highly non-equilibrium switching condition).^{6,19–21} The polarization reversal was studied in slowly increased field with $dE/dt = 2 \text{ kV/mm/min}$ applied using liquid electrodes (LiCl aqueous solution).²²

A Z^+ surface of 0.5-mm-thick congruent lithium tantalate (CLT) and CLN crystals (Oxide Corp., Japan) free of electrodes were irradiated by an IR pulsed CO_2 laser VLS 3.06 (Unique Laser Systems, USA) with $\lambda = 10.6 \mu\text{m}$. A pulse duration of $100 \mu\text{s}$ and an energy density of about 40 J/cm^2 were used for CLT, and a pulse duration of 3 ms and an energy density of about 19 J/cm^2 were used for CLN.

III. ANALYSIS OF THE RAMAN CONFOCAL MICROSCOPY IMAGES

For extracting information about the time evolution of the domain structure at the polar surface, we have analyzed the set of the domain images obtained via Raman confocal microscopy at different depths. The used analysis is based on the following assumptions. First, domain nucleation occurs at the polar surface only. Second, the ratio of sideways domain wall motion velocity to the forward domain growth velocity in the polar direction is constant. In this case, the earlier moments of the domain evolution at the sample polar surface can be restored while going deeper in the bulk (“the earlier, the deeper”) (Fig. 1). The domain images obtained via Raman confocal microscopy at deeper depths (h) correspond to the domain images at the surface at earlier moments

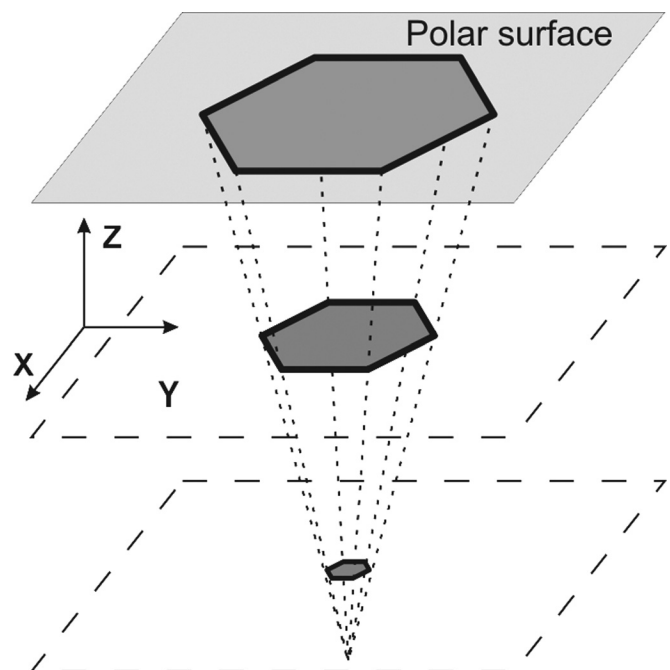


FIG. 1. The principle of the reconstruction of domain evolution. The domain images obtained at different depths correspond to domain patterns at the sample surface at different moments: the deeper the depth, the earlier the moment.

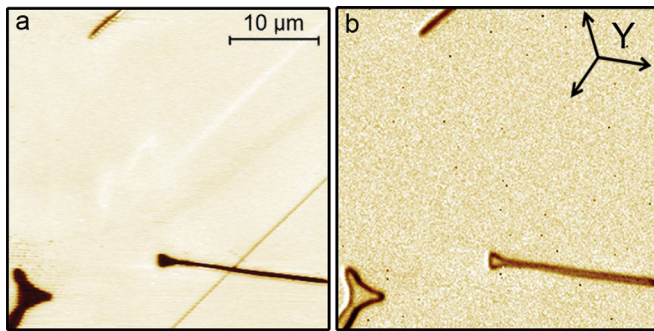


FIG. 2. (Color online) Nanodomain structure at the polar surface in CLN after pulse IR laser irradiation. Visualization by (a) PFM and (b) Raman confocal microscopy.

(t) of the domain structure evolution with the following relation between relative time and relative depth:

$$\frac{h}{h_{\max}} = 1 - \frac{t}{t_{\max}},$$

where h_{\max} is the total domain depth and t_{\max} is the switching time.

Thereby, the images of the static domain structure obtained at the polar surface using classical methods (including PFM) display the final stage only (Fig. 2), and the proposed method enables us to reconstruct the previous stages.

The validity of the made assumptions was confirmed experimentally by the comparison of the *in situ* optical observation of the domain kinetics at the polar surface just after pulse irradiation of the CLN by IR laser²³ and 2D “Raman” domain images obtained while scanning the static final domain structure at different depths (Fig. 3). The optical image has been obtained via a polarizing microscope and was recorded by a high speed video camera (FastCamera13) with a frequency of 400 fps. A CO₂ laser was used for sample irradiation with a single pulse, which allows us to achieve an energy density of about 18 J/cm². Optical images extracted from the video after equal time intervals demonstrate the subsequent arising of three domain rays [Figs. 3(a)–3(c)]. As is seen, these

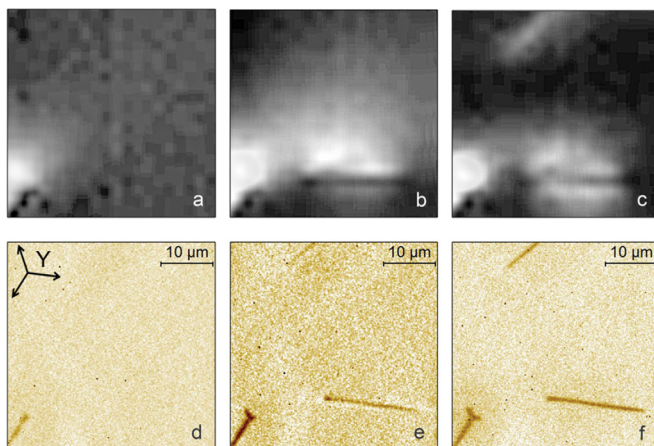


FIG. 3. (Color online) The images of the nanodomain structure formation after pulse IR laser irradiation. Momentary optical images recorded during *in situ* visualization with equal time intervals after IR laser irradiation: (a) 12.5 ms, (b) 30 ms, and (c) 47.5 ms. The domain images obtained via Raman confocal microscopy at different depths from the polar surface: (d) 77 μm, (e) 67 μm, and (f) 57 μm.

images are in one-to-one correspondence with the images obtained with Raman scanning of the static final domain structure at the equidistant depth in the bulk [Figs. 3(d)–3(f)]. The time dependence of the domain length extracted from the image comparison confirms our assumption about the constant domain forward growth velocity. The revealed value of the forward growth velocity is about (600 ± 50) μm/s.

It is necessary to point out that the possibility of extracting information about the domain evolution at the polar surface using the proposed method is lost when the domain reaches the opposite crystal surface.

After that, we analyzed the domain structures formed under highly non-equilibrium switching conditions realized (1) by the application of a uniform field in CLN with the surface layer modified by Ar ion implantation and (2) by the pulse laser irradiation of CLT.

IV. EVOLUTION OF NANODOMAIN RAYS DURING ELECTRIC FIELD POLING IN CLN WITH THE SURFACE LAYER MODIFIED BY AR ION IMPLANTATION

Polarization reversal by electric field poling in CLN samples with a Z⁺ surface layer modified by Ar ion implantation leads to the formation at the unmodified Z⁻ surface of a self-organized domain structure consisting of nanodomain rays mostly oriented along the y-direction. The PFM technique was used to obtain static domain images with a high spatial resolution at the unmodified polar surface (Fig. 4). However, PFM does not provide any information about the domain structure evolution.

Analysis of the Raman confocal images of domains obtained at various depths allows us to separate four consecutive stages of the nanodomain structure evolution at the polar surface (Fig. 5).

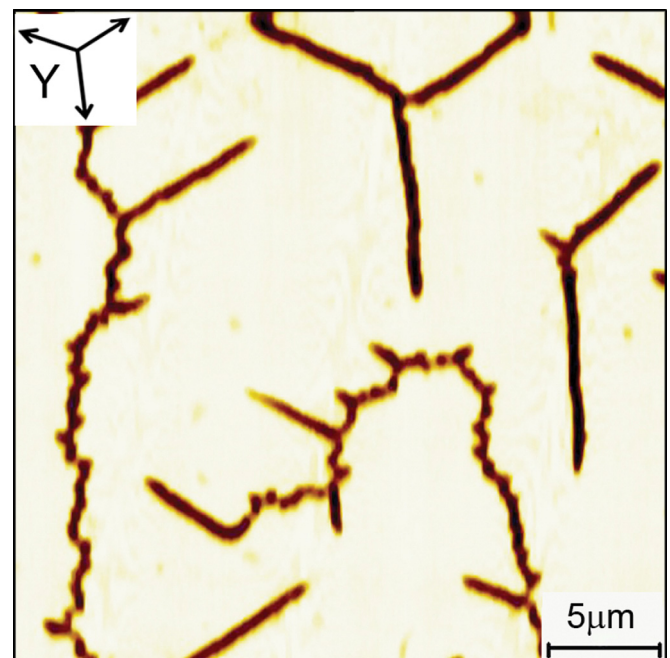


FIG. 4. (Color online) PFM image of nanodomains that appeared at the Z⁻ polar surface in CLN with the Z⁺ surface layer modified by Ar ion implantation. Applied field = 8 kV/mm.

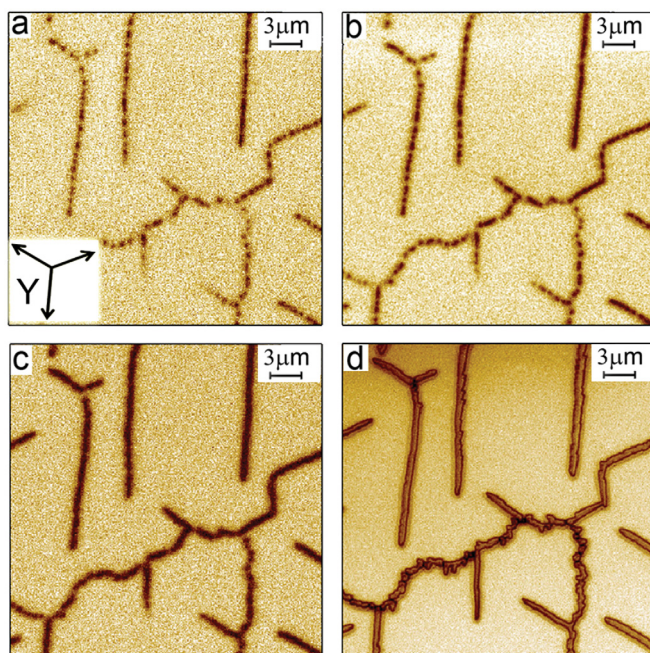


FIG. 5. (Color online) The main stages of the nanodomain structure formation during electric field poling of non-through domains in CLN with the Z^+ surface modified by Ar ion implantation; the images were obtained via Raman confocal microscopy. (a) Nucleation (depth = 34 μm). (b) Sideways growth (depth = 29 μm). (c) Merging (depth = 19 μm). (d) Widening (at the Z^- surface).

The first stage—“nucleation”—represents 1D growth of domain chains (“elongation”), and this has occurred with the formation of a trunk consisting of isolated nanodomains [Fig. 5(a)].

The second stage—“sideways growth”—represents 2D sideways growth of arisen isolated nanodomains [Fig. 5(b)].

The third stage—“merging”—represents the coalescence of growing nanodomains and has occurred with the formation of a solid connected structure of narrow domains [Fig. 5(c)].

The fourth stage—“widening”—represents 1D sideways growth of the formed narrow domains [Fig. 5(d)].

It is interesting to point out that according to our results, the 1D growth of the nanodomain chains (elongation) is almost complete at the end of the first stage, and the domain structure framework is completely formed. This is confirmed experimentally by the fact that the total length of the domain structure remains constant during the following stages.

Two geometrical transitions accompanied by changes of the growth geometry (“geometrical catastrophes”)²⁴ were revealed during the formation of the domain structure. First, the 1D \rightarrow 2D transition occurs at the end of the nucleation stage, when 1D growth of nanodomain chains turns into 2D growth of isolated nanodomains. Second, the 2D \rightarrow 1D transition occurs at the end of the merging stage, when 2D growth of isolated nanodomains turns into 1D growth of solid narrow domains.

V. FORMATION OF NANODOMAIN LATTICE IN CLT AFTER PULSED INFRARED LASER IRRADIATION

The formation of the nanodomain structures after irradiation by pulsed IR laser was studied in CLT. Polarization reversal occurs during cooling after pulse heating under the

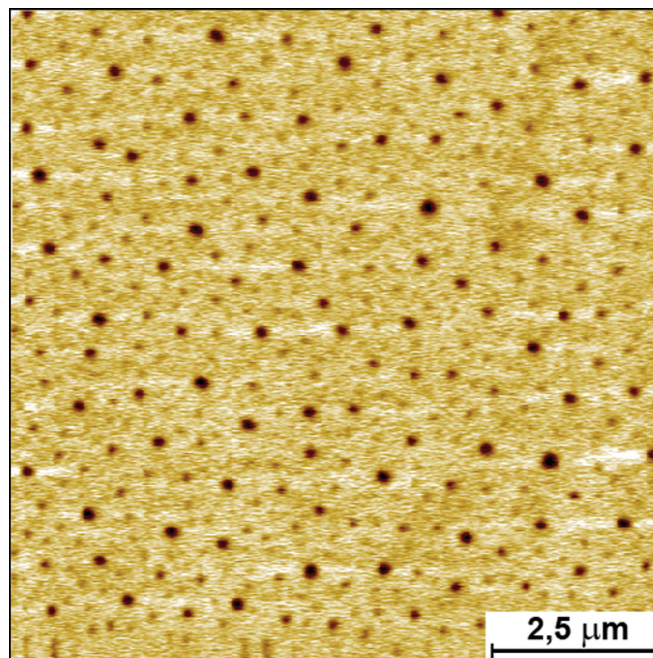


FIG. 6. (Color online) PFM image of isolated nanodomains formed at the irradiated surface after the irradiation of CLT by pulsed IR laser.

action of a pyroelectric field, without any application of an external electric field.²⁵

After single pulse irradiation with an energy density of about 40 J/cm², a self-assembled ensemble of isolated nanodomains appears at the Z^+ surface in the irradiated area of about 1 mm². A PFM image of the irradiated area demonstrates the nanodomains of different sizes with an average density of about 5 μm^{-2} (Fig. 6).

The developed method for nanodomain visualization in the bulk of CLN crystals via analysis of the Raman confocal microscopy data has been adopted by us for CLT. Typical images of the nanodomain structures observed at different depths in CLT are presented in Fig. 7. The analysis of the images, described in the previous section, allowed us to reconstruct the temporal sequence of the isolated nanodomain appearance at the irradiated polar surface.

In the beginning of the switching process, the rhombohedral lattice of isolated nanodomains with a period of about (1800 \pm 200) nm appears [Fig. 7(a)]. Later, the appearance of the nanodomains of the second generation leads to the effect of “spatial frequency doubling” [Fig. 7(b)]. These nanodomains are equally spaced from the first generation ones. Thus, the new lattice with a half period [about (900 \pm 200) nm] appears gradually.

VI. DISCUSSION

The formation of the two types of discrete domain structures—a nanodomain lattice in CLT and nanodomain chains in CLN—in the beginning of the switching process can be understood by taking into account the peculiarities of the local field distribution in the vicinity of an ensemble of needle-like nanodomains with charged walls. The evaluation of the spatial distribution of the electric field shows essential differences close to the needle-like nanodomain and far from it.

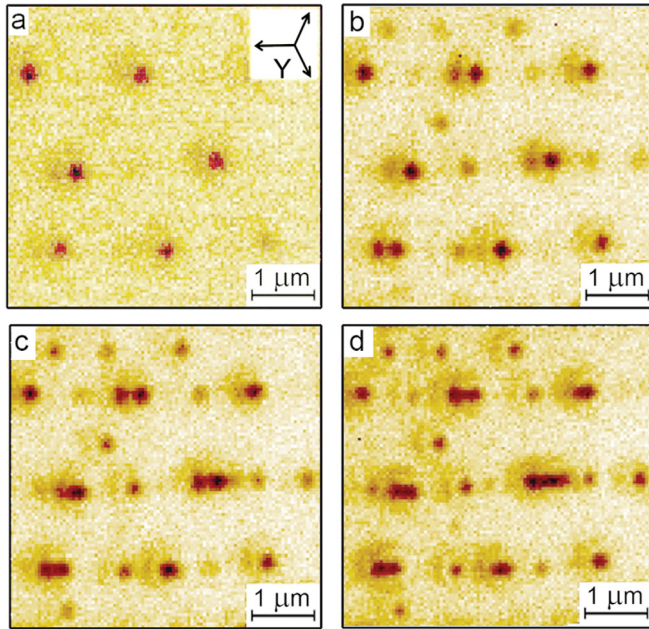


FIG. 7. (Color online) Visualization of the final static nanodomain structure obtained in CLT after pulse IR laser irradiation via Raman confocal microscopy at the different depths: (a) 12.5 μm , (b) 8.4 μm , (c) 4.2 μm , and (d) at the surface.

In the case of the screening retardation when the nucleation at the wall is suppressed, such behavior favors nucleation at short distance in front of the wall (“correlated nucleation”).^{6,7} The formation of the ensembles of isolated nanodomains (“discrete switching”) is observed in such highly non-equilibrium switching conditions.^{6,7,20} It has been shown that this effect leads to the arising of the oriented quasi-periodic chains (arrays) of nanodomains as a result of pulse laser irradiation in CLN.^{21,23,25}

The field produced by the charge walls far from the needle-like domain suppresses the nucleation and hinders the sideways growth of individual domains.^{6,7} This effect leads to the formation of quasi-regular nanodomain lattices.

It is interesting to note that according to our results, the two observed geometrically different nanodomain structures—rays and lattices—are both formed as a result of discrete switching through the arising of correlated ensembles of isolated nanodomains.

The high resolution images obtained via PFM provide information about the final stage of the domain structure evolution at the polar surface only (Fig. 2). The important information about the stages of the domain structure formation is unavailable. In contrast, the proposed method based on the analysis of the images obtained via Raman confocal microscopy at different depths allows us to extract the peculiarities of the domain structure evolution from the beginning to the end in LN and LT in various switching conditions (Figs. 5 and 7). As the earlier stages of the domain structure formation determine the main geometrical parameters of the created domain pattern, the application of this method is crucial for micro- and nanodomain engineering.^{1,2}

It has been shown that the effect of correlated nucleation is typical for polarization reversal in highly non-equilibrium switching conditions and has been observed also in LN after

pulsed laser irradiation.^{21,23,25} The field maximum at a distance of about the length of an isolated needle-like domain has been found experimentally and through computer simulation.^{2,20} The effect of the correlated nucleation is proposed to be the key mechanism for the observed formation of the nanodomain chains.

VII. CONCLUSIONS

Piezoelectric force microscopy and Raman confocal microscopy have been used to study the nanodomain structures in LN and LT crystals. The high-resolution nanodomain images observed at the surface using PFM were supplemented by the domain images at different depths in the crystal bulk obtained via Raman confocal microscopy. It has been shown experimentally that the nanodomain images obtained at different depths in the bulk correspond to domain images at the polar surface obtained at different moments. Such a correlation allows us to reconstruct the main stages of a non-through nanodomain structure evolution at the polar surface.

Using the proposed method, we have separated four consecutive stages—nucleation, sideways growth, merging, and widening—and have revealed two geometrical catastrophes accompanied by changes of the domain growth geometry in LN with a surface layer modified by Ar implantation.

The spatial frequency doubling effect was revealed during the formation of the self-assembled nanodomain structure in CLT after pulse irradiation by infrared laser.

According to our results, the geometrically different nanodomain structures observed in CLT and CLN are both formed as a result of discrete switching through the arising of correlated ensembles of isolated nanodomains.

The unique information about the formation of the nanodomain structures obtained from Raman confocal images is very important for nanodomain engineering and domain wall engineering. This knowledge promises to improve the quality of submicron periodic domain structures for nonlinear-optical devices. The periodical structures in LN and LT produced with nanoscale precision allow one to realize quasi-phase matching, which is an attractive technique for compensating phase velocity dispersion in frequency conversion.

ACKNOWLEDGMENTS

The research was made possible in part by RFBR (Grants 10-02-96042-r-Ural-a, 10-02-00627-a, and 11-02-91066-CNRS-a), by the Ministry of Education and Science: Contract 16.552.11.7020 and the Program “Scientific and scientific-pedagogical personnel of innovative Russia 2009–2013” (Contracts P870, P1262, 14.740.11.0478, and 16.740.11.0585).

¹V. Ya. Shur, in *Handbook of Advanced Dielectric, Piezoelectric and Ferroelectric Materials: Synthesis, Properties and Applications*, edited by Z.-G. Ye (Woodhead Publishing Ltd., Cambridge, England, 2008), pp. 622–669.

²V. Ya. Shur, *Ferroelectrics* **399**, 97 (2010).

³R. L. Byer, *J. Nonlinear Opt. Phys. Mater.* **6**, 549 (1997).

⁴D. S. Hum and M. M. Fejer, *C. R. Phys.* **8**, 180 (2007).

⁵J. A. Armstrong, N. Bloembergen, J. Ducuing, and P. S. Perlsan, *Phys. Rev.* **127**, 1918 (1962).

⁶V. Ya. Shur, *J. Mater. Sci.* **41**, 199 (2006).

⁷V. Ya. Shur, A. L. Gruverman, and E. L. Rumyantsev, *Ferroelectrics* **111**, 123 (1990).

- ⁸W. J. Merz, *Phys. Rev.* **95**, 690 (1954).
- ⁹V. Ya. Shur and E. L. Rumyantsev, *Ferroelectrics* **151**, 171 (1994).
- ¹⁰N. Ohnishi and T. Iizuka, *J. Appl. Phys.* **46**, 1063 (1975).
- ¹¹V. Ya. Shur, A. I. Lobov, A. G. Shur, S. Kurimura, Y. Nomura, K. Terabe, X. Y. Liu, and K. Kitamura, *Appl. Phys. Lett.* **87**, 022905 (2005).
- ¹²A. Gruverman and S. V. Kalinin, *J. Mater. Sci.* **41**, 107 (2006).
- ¹³B. J. Rodriguez, R. J. Nemanich, A. Kingon, A. Gruverman, S. V. Kalinin, K. Terabe, X. Y. Liu, and K. Kitamura, *Appl. Phys. Lett.* **86**, 012906 (2005).
- ¹⁴R. C. Miller and A. Savage, *Phys. Rev. Lett.* **2**, 294 (1959).
- ¹⁵R. Hammoum, M. D. Fontana, P. Bourson, and V. Ya. Shur, *Appl. Phys. A* **91**, 65 (2008).
- ¹⁶P. S. Zelenovskiy, M. D. Fontana, V. Ya. Shur, P. Bourson, and D. K. Kuznetsov, *Appl. Phys. A* **99**, 741 (2010).
- ¹⁷V. Ya. Shur, E. I. Shishkin, E. V. Nikolaeva, M. S. Nebogatikov, D. O. Alikin, P. S. Zelenovskiy, M. F. Sarmanova, and M. A. Dolbilov, *Ferroelectrics* **398**, 91 (2010).
- ¹⁸P. Capek, G. Stone, V. Dierolf, C. Althouse, and V. Gopalan, *Phys. Status Solidi* **4**, 830 (2007).
- ¹⁹V. Ya. Shur, E. L. Rumyantsev, E. V. Nikolaeva, E. I. Shishkin, D. V. Fursov, R. G. Batchko, L. A. Eyres, M. M. Fejer, R. L. Byer, and J. Sindel, *Ferroelectrics* **253**, 105 (2001).
- ²⁰V. Ya. Shur, D. K. Kuznetsov, A. I. Lobov, E. V. Nikolaeva, M. A. Dolbilov, A. N. Orlov, and V. V. Osipov, *Ferroelectrics* **341**, 85 (2006).
- ²¹V. Ya. Shur, E. L. Rumyantsev, E. V. Nikolaeva, E. I. Shishkin, D. V. Fursov, R. G. Batchko, L. A. Eyres, M. M. Fejer, and R. L. Byer, *Appl. Phys. Lett.* **76**, 143 (2000).
- ²²D. O. Alikin, E. I. Shishkin, E. V. Nikolaeva, V. Ya. Shur, M. F. Sarmanova, A. V. Ievlev, M. S. Nebogatikov, and N. V. Gavrilov, *Ferroelectrics* **399**, 35 (2010).
- ²³V. Ya. Shur, D. K. Kuznetsov, E. A. Mingaliev, E. M. Yakunina, A. I. Lobov, and A. V. Ievlev, In Situ Investigation Of Formation Of Self-Assembled Nanodomain Structure In Lithium Niobate After Pulse Laser Irradiation, *Appl. Phys. Lett.* (submitted).
- ²⁴V. Ya. Shur, E. L. Rumyantsev, and S. D. Makarov, *J. Appl. Phys.* **84**, 445 (1998).
- ²⁵D. K. Kuznetsov, V. Ya. Shur, E. A. Mingaliev, S. A. Negashev, A. I. Lobov, E. L. Rumyantsev, and P. A. Novikov, *Ferroelectrics* **398**, 49 (2010).